

The Ordered Matrix Dirichlet for Modeling Ordinal Dynamics

Niklas Stoehr
ETH Zurich

Benjamin J. Radford
UNC Charlotte

Ryan Cotterell
ETH Zurich

Aaron Schein
University of Chicago

Abstract

Many dynamical systems exhibit latent states with intrinsic orderings such as “ally”, “neutral” and “enemy” relationships in international relations. Such latent states are evidenced through entities’ cooperative versus conflictual interactions which are similarly ordered. Models of such systems often involve state-to-action emission and state-to-state transition matrices. It is common practice to assume that the rows of these stochastic matrices are independently sampled from a Dirichlet distribution. However, this assumption discards ordinal information and treats states and actions falsely as order-invariant categoricals, which hinders interpretation and evaluation. To address this problem, we propose the Ordered Matrix Dirichlet (OMD): rows are sampled conditionally dependent such that probability mass is shifted to the right of the matrix as we move down rows. This results in a well-ordered mapping between latent states and observed action types. We evaluate the OMD in two settings: a Hidden Markov Model and a novel Bayesian Dynamic Poisson Tucker Model tailored to political event data. Models built on the OMD recover interpretable latent states and show superior forecasting performance in few-shot settings. We detail the wide applicability of the OMD to other domains where models with Dirichlet-sampled matrices are popular (e.g. topic modeling) and publish [user-friendly code](#).

1 Introduction

In many modeling settings and application domains, some aspect of the observation space has an intrinsic ordering. For example, observed political interactions between countries can be ordered by conflict-cooperation intensity, ranging

niklas.stoehr@inf.ethz.ch
ryan.cotterell@inf.ethz.ch
schein@uchicago.edu bradfor7@uncc.edu
<https://github.com/niklasstoehr/ordered-matrix-dirichlet>

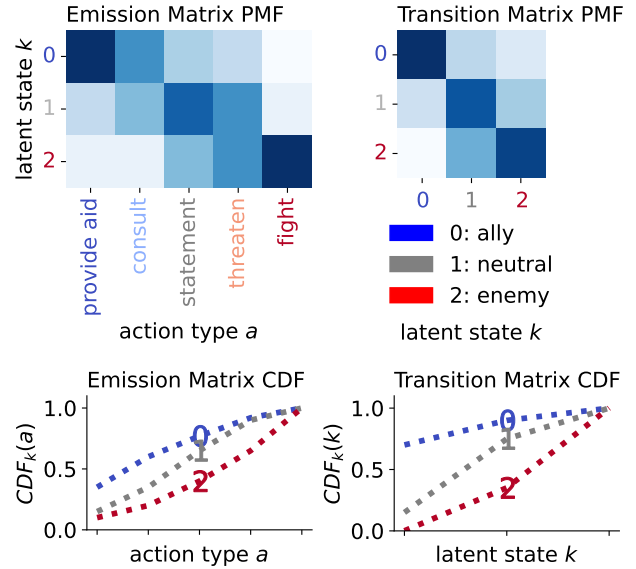


Figure 1: We are dealing with observed states that are naturally ordered such as action types a . Emission matrix: We expect cooperative actions (e.g. “provide aid”) to be associated with more cooperative latent states k (e.g. “ally”). Transition matrix: we expect latent states to transition to adjacent states (e.g. $k = 0$ to $k = 1$). To model these assumptions, the Ordered Matrix Dirichlet (OMD) ensures that each discrete probability distribution per state k has first-order stochastic dominance (FSD) over the next distribution $k + 1$. This constraint is exemplified by non-overlapping cumulative distribution functions for each latent k .

from “provide aid” to “fight” (Goldstein, 1992; Schrodt, 2008). This ordering should ideally be reflected in the latent states driving the observed actions. For example, conflictual actions like “fight” should more likely be observed if countries are in a latent “enemy” state (Schrodt, 2006). In this setting, latent states represent relationship statuses that are ordered due to observed actions, ranging from “ally” to “enemy” states. An additional structural assumption may be that these latent states transition step-by-step through adjacent states. Enemies rarely become allies from one moment to the other, but transition smoothly. These assumptions are a subject of study in international relations (Davis and Stan, 1984; Kalyvas, 2006) and exemplified in Fig. 1.

Many models of dynamical systems rely on the notion of a state-to-action emission matrix and a state-to-state transition matrix such as the prominent Hidden Markov Model (HMM) (Baum and Petrie, 1966) (§2). The matrices’ rows describe discrete distributions that are often sampled independently from a Dirichlet distribution. This however results in the states and actions to be categorical without particular ordering. We refer to the distribution over this kind of stochastic matrices as *Standard Matrix Dirichlet* (SMD) (§3.1). It not only discards ordinal information, but also leads to a problem called label switching (Stephens, 2000): the order-invariance of states complicates interpretability and evaluation with conventional classification metrics.

So how can we reflect the assumption of action and state ordering in our model? One existing idea is to simply constrain the non-zero entries of a matrix to be “banded” along its diagonal (§3.2). However, this *Banded Matrix Dirichlet* (BMD) is inflexible, ruling out a large number of structures such as upper diagonal matrices. Instead, we propose the *Ordered Matrix Dirichlet* (OMD), a distribution over a subset of stochastic matrices with uniquely ordered latent states (§3.3). In particular, the OMD ensures that row k has first-order stochastic dominance over row $k + 1$. This means that probability mass is shifted to the right of the matrix as we move down rows as outlined in Fig. 1.

The OMD as a modeling motif has wide applicability to a broad family of dynamical systems with Dirichlet-sampled matrices as we formalize in §2. In this paper, we focus on two models and two kinds of data: (1) First, we evaluate the OMD within a Hidden Markov Model to recover synthetically generated data with known ordinal dynamics (§5). (2) Second, we consider the application domain of international relations because there exist large political event datasets of human-annotated, ordered interactions as well as a popular understanding of latent relationships between countries (§6.1). Harnessing these complex structures requires an highly expressive novel *Dynamic Poisson Tucker Model* (DPT) that we present in §6.2.

We conduct imputation and forecasting tasks on held-out data. We find that the OMD does not significantly forfeit predictive fit while bringing the benefit of easily interpretable latent representations. In forecasting and settings of data scarcity, the inductive bias of the OMD even improves performance. We review additional models and applications with ordinal dynamics in §7 and discuss related work in §8.

2 Ordered Dynamical System

We are modeling time series observations $y_a^{(t)}$, where t indexes discrete time steps and a indexes observed action types. Importantly, action types are ordered — for instance, political interactions are ordered by conflict-cooperation intensity ranging from “provide aid” to “fight”. For this

kind of data, we describe a canonical family of dynamical system comprising emission and transition matrices. In these models, each observation $y_a^{(t)}$ is modeled as $\mathbb{E}[y_a^{(t)}] = \mu_a^{(t)}$ and decomposes according to

$$\mu_a^{(t)} = \sum_{k=1}^K \lambda_k^{(t)} \underbrace{\phi_{ka}}_{\text{emission}} \quad (1)$$

The parameter ϕ_{ka} represents the relevance of action a in latent state k and forms a state-to-action emission matrix $\Phi \in [0, 1]^{K \times A}$. $\lambda_k^{(t)}$ describes a latent parameter over K latent states and transitions over time based on

$$\lambda_k^{(t)} = \sum_{k_1=1}^K \lambda_{k_1}^{(t-1)} \underbrace{\pi_{k_1 k}}_{\text{transition}} \quad (2)$$

where $\pi_{k_1 k}$ is an element of a state-to-state transition matrix $\Pi \in [0, 1]^{K \times K}$ that evolves latent states from time step $t - 1$ to t . This formulation can be related to a Hidden Markov Model (HMM) or more complex dynamical systems as presented in §6.2.

Ordered State-to-Action Mapping. Note that each row ϕ_k of the emission matrix represents a discrete distribution over A ordered action types on the $(A - 1)$ -simplex — i.e., $\sum_{a=1}^A \phi_{ka} = 1$ and $\phi_{ka} > 0$. Unlike O’Connor et al. (2013); Schein et al. (2015, 2016b), who treat action types and latent states as categorical, we explicitly model ordering: on average, latent state k should be associated with higher ranked actions than state $k - 1$ (Stoehr et al., 2022).

Ordered State-to-State Transitions. Each row π_k in the transition matrix defines a $(K - 1)$ -probability simplex of transitioning to all K latent states from state k . One may wish to constrain latent states to transition smoothly to neighboring states and to itself instead of immediately jumping from low-rank to high-rank states within a single time step. This gradual (de-)escalation is typically achieved by constraining the transition matrix Π (Schrodt, 2006; Netzer et al., 2008; Anders, 2020; Randahl and Vegelius, 2022).

3 Stochastic Matrix Construction

3.1 Standard Matrix Dirichlet (SMD)

The conventional way of constructing a stochastic matrix is to sample each row ϕ_k independently from a Dirichlet distribution. We term the distribution over this standard kind of stochastic matrices the Standard Matrix Dirichlet (SMD). As outlined in Fig. 2, SMD does not necessarily adhere to any desired ordering constraints, previously outlined in §2.

3.2 Banded Matrix Dirichlet (BMD)

A simple trick to obtain some row ordering is to limit the non-zero elements to be *banded* along the matrix’ diagonal

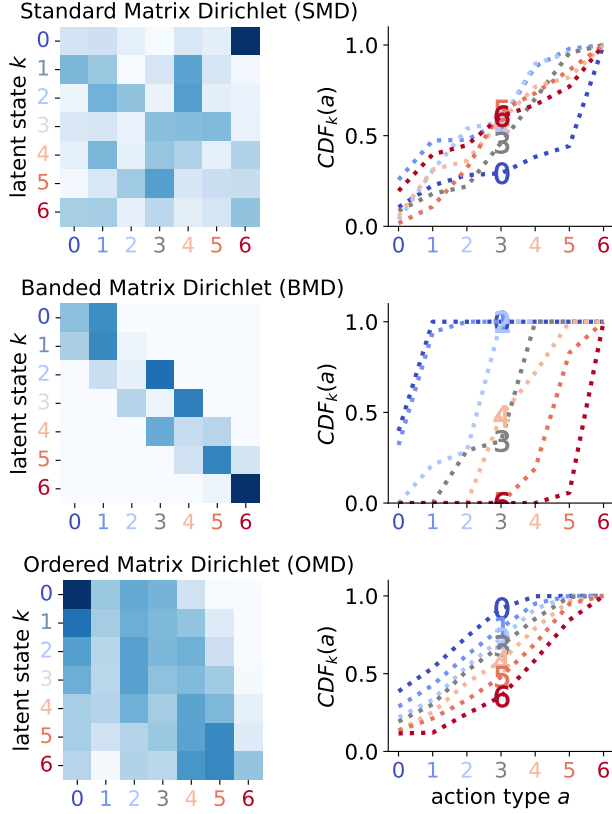


Figure 2: Stochastic matrices sampled from the Standard Matrix Dirichlet (SMD), Banded Matrix Dirichlet (BMD) and Ordered Matrix Dirichlet (OMD) distribution. Neither the SMD nor the OMD are necessarily adhering to the First-order Stochastic Dominance (FSD) constraint. This can be seen from overlapping cumulative distribution functions (CDF) for each row / latent state. In both, the SMD and BMD, rows can be switched.

(see the middle plot of Fig. 2). This is referred to as Banded Matrix Dirichlet (BMD) or left-to-right matrix (Schrodt, 2006; Subakan et al., 2015). For instance, in the transition matrix proposed by Schrodt (2006); Randahl and Vegelius (2022), the k^{th} state can only be excited by its adjacent states, $(k-1)^{\text{th}}$ and $(k+1)^{\text{th}}$, as well as by itself. We can consider a wider bandwidth $b \geq 1$ so that components $k' \in \{k-b, \dots, k+b\}$ all excite k .¹ However, the BMD is still very restrictive and a unique, monotonic ordering of rows is not ensured as can be seen in Fig. 2.

3.3 Ordered Matrix Dirichlet (OMD)

What is a more flexible construction realizing the structural constraints described in §2? We propose a constraint based on *First-order Stochastic Dominance* (FSD). Then, we bake this constraint into a stick-breaking construction for

¹Throughout this work, we consider $b = 1$.

Algorithm 1 Ordered Matrix Dirichlet

```

1: Input: alpha concentration prior  $\alpha \in \mathbb{R}_+^A$ 
2: for  $k = 1, \dots, K$  do
3:    $\tilde{\phi}_{k1} \stackrel{\text{iid}}{\sim} \text{Beta}(\alpha_1, \sum_{a=2}^A \alpha_a)$ 
4: end for
5:  $(\tilde{\phi}_{11}, \dots, \tilde{\phi}_{K1}) \leftarrow \text{SORT}((\tilde{\phi}_{11}, \dots, \tilde{\phi}_{K1}))$ 
6: for  $a = 2, \dots, A-1$  do
7:   for  $k = 1, \dots, K$  do
8:      $\tilde{\beta}_{ka} \stackrel{\text{iid}}{\sim} \text{Beta}(\alpha_a, \sum_{a'=a+1}^A \alpha_{a'})$ 
9:   end for
10:   $(\tilde{\beta}_{1a}, \dots, \tilde{\beta}_{Ka}) \leftarrow \text{SORT}((\tilde{\beta}_{1a}, \dots, \tilde{\beta}_{Ka}))$ 
11:  for  $k = 1, \dots, K$  do
12:     $\phi_{ka} \leftarrow (1 - \sum_{a'=1}^{a-1} \phi_{ka'}) \tilde{\beta}_{ka}$ 
13:  end for
14: end for
15: for  $k = 1, \dots, K$  do
16:    $\phi_{kA} \leftarrow 1 - \sum_{a'=1}^{A-1} \phi_{ka'}$ 
17: end for
18: Output: OMD variate  $\Phi \in \mathbb{R}_+^{K \times A}$ 

```

sampling variates from a distribution over FSD-constrained stochastic matrices that we coin *Ordered Matrix Dirichlet*.

First-order Stochastic Dominance (FSD). We restrict the discrete distribution ϕ_k to have First-order Stochastic Dominance (FSD) over ϕ_{k+1} .² which imposes an ordering over the matrices' rows according to

$$\sum_{a=1}^{\ell} \phi_{ka} \geq \sum_{a=1}^{\ell} \phi_{(k+1)a} \text{ for all } \ell \in \{1, \dots, A\} \quad (3)$$

In particular, ϕ_k dominates ϕ_{k+1} if its cumulative distribution function $\text{CDF}_k(a)$ at each point a is higher than or equal to $\text{CDF}_{k+1}(a)$ (Massey, 1987) following

$$\text{CDF}_k(a) = \sum_{a'=1}^a \phi_{ka'} \quad (4)$$

$$\text{CDF}_k(a) \geq \text{CDF}_{k+1}(a) \text{ for all } a \quad (5)$$

Stick-Breaking Construction. We can generate a Dirichlet random variate by relying on a stick-breaking algorithm (Gelman et al., 2013, p. 585) (Algorithm 1). Stick-breaking (Sethuraman, 1994) iteratively partitions (breaks) a line (stick) into parts. The size (length) of the broken part is determined by sampling from a Beta distribution.

Using this construction, we can independently sample K Dirichlet distributions. This is exemplified by the for-loop of length K in lines 2, 7 and 15 of Algorithm 1. In fact, if we omitted lines 5 and 10 in Algorithm 1, the algorithm

²Note that the FSD constraint transfers to matrices of any shape, such as the square $K \times K$ transition matrix $\mathbf{\Pi}$.

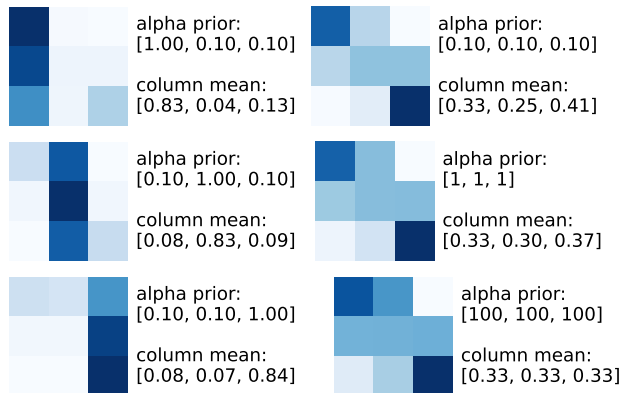


Figure 3: Ordered Matrix Dirichlet with different alpha concentration priors $\alpha \in \mathbb{R}_+^A$ averaged over $N = 10000$ samples. Column mean corresponds to $\bar{\phi}_a = \frac{1}{K} \sum_{k=0}^K \phi_{k,A}$ and shows that probability mass is asymmetric to the right.

would return a sample from the Standard Matrix Dirichlet (SMD). Yet, the sorting causes the K discrete distributions to be dependent. Note that sorting only marginally increases time complexity from $\mathcal{O}(A \times K)$ to $\mathcal{O}(A \times K \log K)$. Importantly, the sorting ensures that the $(k + 1)^{\text{th}}$ distribution is bounded by the k^{th} . Due to this constraint, distributions ϕ_k are not sampled from a Dirichlet anymore, but are constrained simplex vectors. The algorithm returns a variate from a distribution over FSD-constrained matrices.

Alpha Concentration Prior. The OMD is parametrized by an alpha concentration vector $\alpha \in \mathbb{R}_+^A$. Fig. 3 visualizes the effect that different configurations of α have on Φ . For symmetric α , one typically expects the probability mass to be symmetric as in the Dirichlet distribution. In the case of the OMD, we observe that probability mass is slightly asymmetric to the right, particularly for higher values of α_a . This is due to the sorting operation that returns the K^{th} order statistics of a Beta-distributed variable as elaborated in App. A. However, this does not mean that the OMD is inherently asymmetric. There exist infinitely many settings of α values that induce symmetry. These values can be learned during posterior inference. Thus, the asymmetry has no negative consequences on the flexibility of the OMD.

Label switching proposition. The First-order Stochastic Dominance constraint mitigates the label switching problem (Stephens, 2000) of order-invariant latent states (see appendix Fig. 11). Previous work has shown that the parameters of Hidden Markov Models (and admixture models (Hillar and Sommer, 2011)) are identifiable up to permutation of the latent states (Allman et al., 2009, p. 3123). By definition, there exists a single ordering of random variables under the FSD constraint (Hadar and Russell, 1969). In turn, the FSD-bounded rows of the OMD have a unique ordering. Importantly, we consider imposing structure in both the

emission and the transition matrix. However, to ensure this unique ordering of latent states, it suffices that the rows of the emission matrix Φ are ordered. The ordering perpetuates and affects the ordering of rows and columns in the transition matrix Π alike. Constraining Π serves the purpose of imposing (de-)escalatory transition dynamics.

4 Technical Details

4.1 Implementation and Inference

The Ordered Matrix Dirichlet integrates nicely with the available tools in probabilistic programming. We implement the OMD in a few lines using the probabilistic programming API *Pyro* (Bingham et al., 2018; Phan et al., 2019).³ Our construction algorithm only involves the sorting of samples from a Beta distribution. This does not obstruct the computation of gradients (Blondel et al., 2020) and enables gradient-based optimization methods, such as Hamiltonian Markov Chain Monte Carlo (HMC) and Stochastic Variational Inference (SVI) for posterior inference. To infer posterior parameters, we run the HMC-variant *No-U-Turn Sampler (NUTS)* (Duane et al., 1987; Homan and Gelman, 2014) to take $S = 1000$ posterior after 200 warm-up samples. This takes about 30 minutes on a single NVIDIA TITAN RTX GPU core.

4.2 Predictive Evaluation Methodology

Prediction Tasks. We evaluate the inferred posterior parameters in two predictive tasks on a held-out testing set:

- (1) Imputation: we randomly select, remove and mask 30% of the entries in the full count tensor. For evaluation, we consider a testing set which consists of the full, unmasked tensor. However, we evaluate model predictions only on the previously masked event entries.
- (2) Forecasting: we split the time series by time: the first 70% serve as training and the latter 30% as testing data.

Evaluation Metrics. We consider two evaluation metrics:

- (1) As a density-based metric, we compute the posterior predictive density (PPD) (Gelman et al., 1996) following $\exp \frac{1}{N} \sum_{n=0}^N \log(\sum_s^S p(y_n | \theta^{(s)}))$.⁴ PPD ranges between 0 and ∞ and measures the averaged log-likelihood of the held-out data given the inferred posterior parameters $\theta^{(s)}$.
- (2) As a point estimate-based metric, we consider the mean absolute error (MAE). To predict the posterior mean \hat{y}_n , we compute $\mathbb{E}[y_n^{(s)} | \theta^{(s)}] \sim \frac{1}{S} \sum_{s=1}^S y_n^{(s)}$.⁴

³We open-source our code jointly with tutorials and examples on how to use the OMD within popular models.

⁴ $y_n = y_a^{(t)}$ or in the case of the 4-mode count tensor introduced in §6.1, $\mathbf{n} = (i, j, a, t)$ is a multi-index such that $y_n = y_{i \rightarrow j}^{(t)}$.

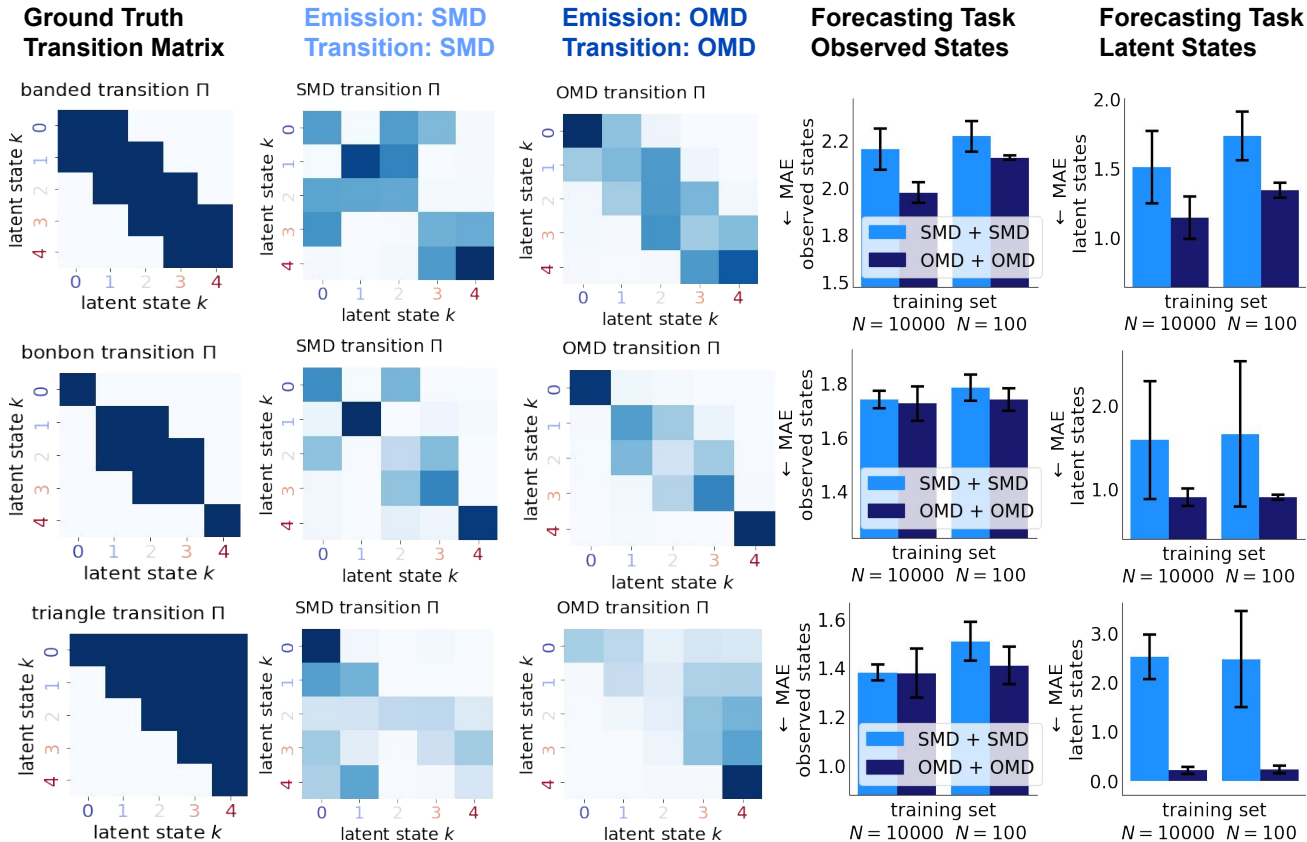


Figure 4: Forecasting comparison between the SMD and the OMD as transition and emission matrix in an Hidden Markov Model (HMM). We synthetically generate data using different ground truth transition matrices (left column). We use a noisy diagonal matrix as ground truth emission matrix. The OMD does a better job at recovering ground truth transitions as the SMD (center (left)). The OMD performs en par with SMD at predicting observed states and even wins in few-shot settings ($N = 100$) (center right). OMD consistently outperforms SMD in predicting latent states due to label switching (right).

5 Synthetic Data Experiments

We generate synthetic data using a Hidden Markov Model with known parameters. For the emission matrix, we consider a noisy diagonal matrix. For the transition matrix, we experiment with different transition patterns: “banded”, “bonbon” and “triangle”, all displayed in the left column of Fig. 4. The “bonbon” pattern, for instance, represents a realistic scenario for political event data, where “neutral” states fluctuate but “ally” and “enemy” states are absorbing. Using these matrices as ground truth parameters, we generate $N = 10000$ sequences of length $T = 10$.

For training and testing, we consider two settings: SMD + SMD and OMD + OMD. For instance, SMD + SMD refers to the parametrization of the HMM’s emission and transition matrix using the SMD. Next, we fit the model and inspect whether learned transition patterns recover the ground truth, displayed in columns 2 and 3 of Fig. 4. Considering the ground truth of the “triangle transition” in the bottom row for instance: SMD confuses the correct upper triangle structure with a lower triangle. This exemplifies the label switching

problem. In contrast, all ground truth transition patterns are clearly captured by the OMD.

Generating synthetic data has the advantage that we know the ground truth latent states at each time step, allowing for a quantitative evaluation of inferred latent states. We consider one setting with all $N = 10000$ sequences and a few-shot setting with $N = 100$ sequences. Inspecting columns 4 and 5 of Fig. 6, two results are standing out: Firstly, when forecasting observed states, the OMD + OMD consistently outperforms the more flexible SMD + SMD in the few-shot setting of $N = 100$. The inductive bias of the OMD is picking up the ground truth structures more quickly.

Secondly, when predicting latent states, OMD + OMD clearly wins in all settings. The reason for this lies in the label switching of latent states. This is also reflected in the high standard deviation of the MAE over the 10 runs with different random seeds. For SMD + SMD, the labels of the latent states are switched for every run, resulting in volatile results. We repeat these synthetic data experiments for the imputation setting (see Fig. 12 in the appendix).

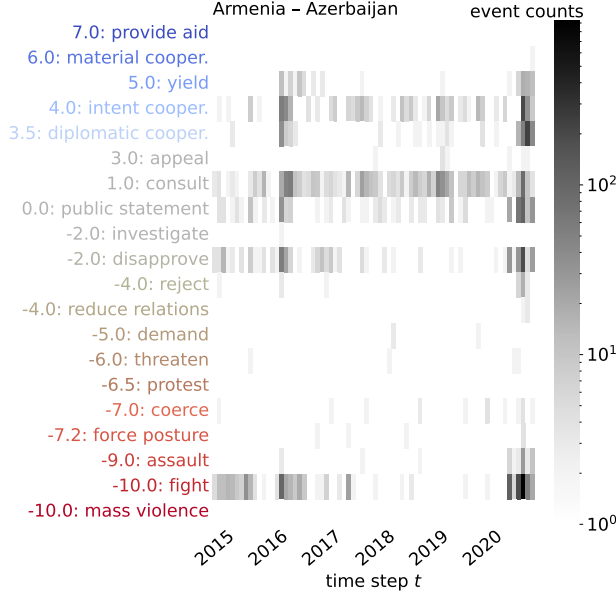


Figure 5: Subset of ICEWS event data showing how country interactions are changing smoothly over time. The full event tensor is of shape $I \times J \times A \times T$ and represents actions a exchanged between countries i and j at time step t . Here, we display Armenia and Azerbaijan, aggregated by months.

6 Case Study: International Relations

6.1 Dyadic Political Events Dataset

Ordered Action Types. We consider the political event dataset *Integrated Crisis Early Warning System (ICEWS)* (Boschee et al., 2015), in particular the *ICEWS Coded Event Data*. ICEWS is one of the largest collections of country-level “who-did-what-to-whom-at-what-time” quadruplets. All events are annotated with a timestamp, source and target country and an action type. Action types and actors are machine-coded by Raytheon BBN’s ACCENT software into the *Conflict and Mediation Event Observations (CAMEO)* ontology (McClelland, 1984; Schrodt et al., 2008; Schrodt, 2012). CAMEO specifies 20 high-level action types, listed on the left in Fig. 5. The *Goldstein Scale* (Goldstein, 1992) provides an expert-based conflict-cooperation intensity ranking of these action types. For instance, “use unconventional mass violence” and “fight” are ranked most conflictual (both -10.0) and “provide aid” ($+7.0$) most cooperative.

4-mode Count Tensor. We omit all self-targeted events where the source and target country are the same and select the time period from 2015 to 2020 which leaves us with 1,833,552 events in total. The data can be organized into a 4-mode count tensor $\mathbf{Y} \in \mathbb{Z}_0^{I \times J \times A \times T}$ where an element $y_{i \rightarrow j}^{(t)}$ describes the number of times country i took action a to country j during time step t . We consider $I = 249$ source and $J = 249$ target countries, $A = 20$ action types ordered

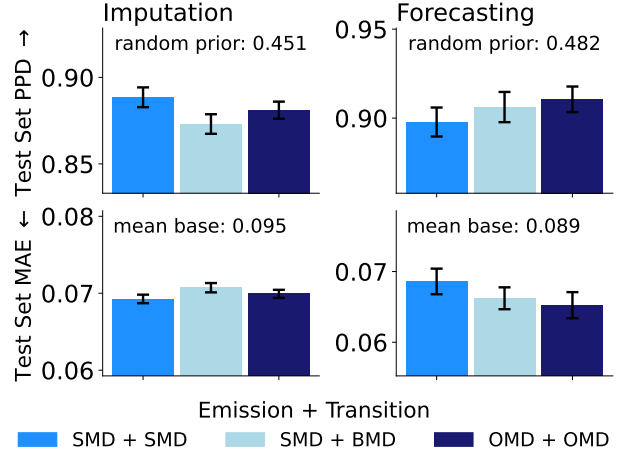


Figure 6: Imputation and forecasting evaluation on held-out ICEWS data, over 10 runs with random seed. We fit the DPT model with different parametrizations (SMD, BMD, OMD) of the emission Φ and transition Π matrix. We find that OMD does not significantly reduce predictive results suggesting that the imposed constraints fit the given data.

by the Goldstein scale and $T = 72$ time steps, aggregating onto a temporal granularity of months. A slice of this count tensor showing interactions between $i = \text{Armenia}$ and $j = \text{Azerbaijan}$ is presented in Fig. 5.

6.2 Dynamic Poisson Tucker Model

We present the OMD as the empowering motif within a highly expressive model tailored to count-based political event data. To this end, we extend the dynamical system presented in §2 by augmenting the likelihood of Eq. (1) and the transition dynamics of Eq. (2). We model the counts $y_{i \rightarrow j}^{(t)}$ of the 4-mode tensor \mathbf{Y} to be Poisson-distributed:

$$y_{i \rightarrow j}^{(t)} \sim \text{Pois} \left(\delta_a \delta^{(t)} \sum_{k=1}^K \lambda_{i \rightarrow j}^{(t)} \underbrace{\phi_{ka}}_{\text{emission}} \right) \quad (6)$$

$\delta_a \in \mathbb{R}_+^A \sim \text{Gamma}(\alpha_a, \beta_a)$ and $\delta^{(t)} \in \mathbb{R}_+^T \sim \text{Gamma}(\alpha_t \delta^{(t-1)}, \alpha_t \beta_t)$ are (optional) action and time scaling coefficients. $\delta^{(t)}$ accounts for changes in the number of reported events over time. The model is said to be stationary if $\delta^{(t)} = \delta$ for $\forall t = \{1, \dots, T\}$. Instead of modeling latent states k between countries i and j , we can model the rate at which countries in community c_1 take actions in state k towards countries in community c_2 during time step t . To this end, we apply *Tucker Decomposition* (Tucker, 1964):

$$\sum_{k=1}^K \lambda_{i \rightarrow j}^{(t)} \phi_{ka} = \sum_{c_1=1}^C \sum_{c_2=1}^C \sum_{k=1}^K \psi_{c_1 i} \psi_{c_2 j} \phi_{ka} \lambda_{c_1 \rightarrow c_2}^{(t)}$$

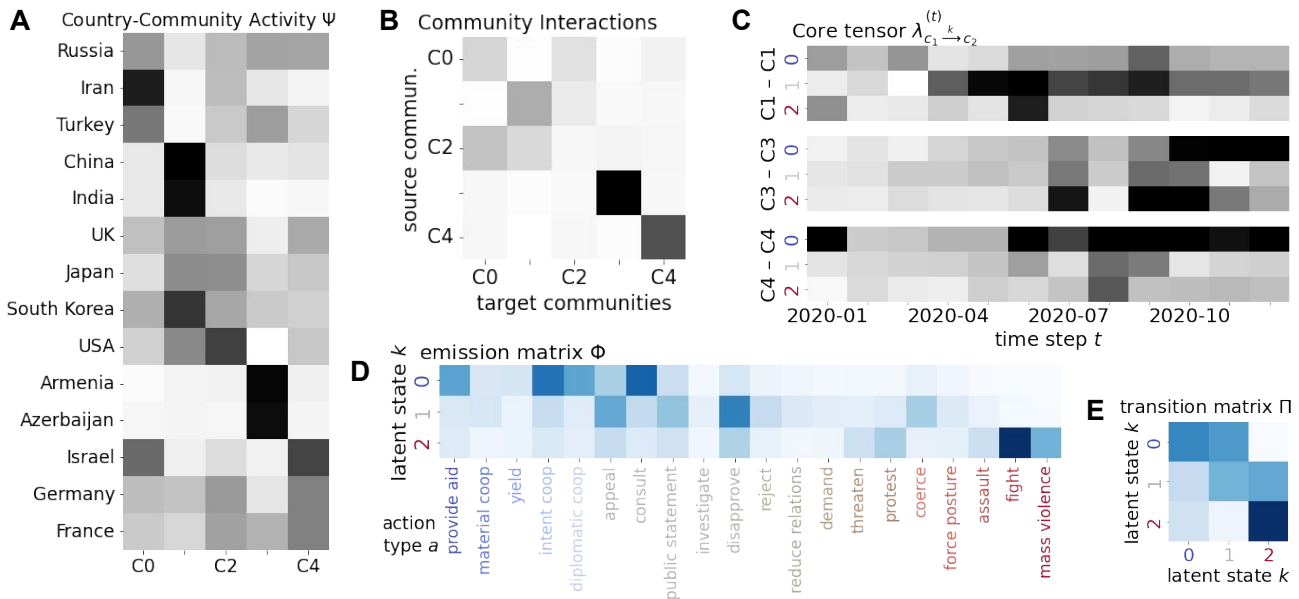


Figure 7: Posterior parameters of Dynamic Poisson Tucker Model fitted to ICEWS subset of 2020. (A) The latent matrix Ψ indicates country-community activity. Armenia and Azerbaijan are standing out as they are involved in one community only (B) Interactions between latent communities. We find that communities C3 and C4 predominantly interact between themselves. (C) Selected community interactions over time: C3-C3 are in conflict, while C4-C4 are mostly friendly. (D) Latent emission matrix Φ representing global state-to-action probabilities. Thanks to the ordering, we know that state $k = 2$ represents conflictual relationships. (E) Latent transition matrix Π representing smooth state-to-state transition probabilities.

where $\lambda_{c_1 \rightarrow c_2}^{(t)}$ forms the *core tensor* $\Lambda^{(t)} \in \mathbb{R}_+^{C \times C \times K}$. The parameter $\psi_{c_1 i}$ represents the rate at which country i acts as a source in community c_1 , analogously $\psi_{c_2 j}$ represents country j as a target in community c_2 . Both parameters are gamma-distributed, e.g. $\psi_{c_1 i} \sim \text{Gamma}(\alpha_i, \beta_i)$, and describe a community-country matrix $\Psi \in \mathbb{R}_+^{C \times V}$.

Finally, we adjust the transition dynamics expressed in Eq. (2) to be Gamma-distributed. In doing so, we follow the Poisson–Gamma Dynamical System (Schein et al., 2016b, 2019) and set the hyperparameter τ_0 to 1 as shown below.

$$\lambda_{c_1 \rightarrow c_2}^{(t)} \sim \text{Gam} \left(\tau_0 \sum_{k_1=1}^K \lambda_{c_1 \rightarrow c_2}^{(t-1)} \underbrace{\pi_{k k_1}}_{\text{transition}}, \tau_0 \right)$$

6.3 Experiments and Results

Predictive Evaluation. We quantitatively evaluate the performance of the SMD, BMD and OMD within the Dynamic Poisson Tucker Model with $C = 5$ and $K = 3$. To this end, we choose different combinations of parametrizations for the emission and transition matrices, listed in the legend of Fig. 6. The imputation results reflect that the SMD is indeed more flexible than the OMD, which, in turn, is more flexible than the BMD. However, imputation does not necessarily require a model with a temporal component as it is required in forecasting. In forecasting, SMD + SMD is outperformed by OMD + OMD. The latter can be con-

sidered a stable, low-variance predictor that learns smooth state transitions and is less likely to zoom off into “wild states”. Overall however, we can conclude that prediction performance differs only very marginally. This suggests that the FSD-constraint enforced by the OMD (and BMD) is indeed suited for the data at hand. Using the OMD, we potentially forfeit little predictive performance, while gaining interpretable latent structure as outlined next.

Descriptive Evaluation. We fit the DPT model with $C = 5$ and $K = 3$ to the ICEWS event dataset and inspect the posterior parameters of the latent variables. Importantly, we parameterize the emission and transition matrix using the Ordered Matrix Dirichlet. Fig. 7 shows the time period of 2020.⁵ Fig. 7A visualizes country-community activity Ψ . We observe that Armenia and Azerbaijan are predominantly involved in community C3. This community is mostly interacting with itself as can be seen in Fig. 7B. Moreover, the state of interaction is conflictual as shown in Fig. 7C. We know that latent state $k = 2$ corresponds to a conflictual relationship thanks to the well-ordered emission matrix Φ of state-to-action probabilities (see Fig. 7D). Without this ordering constraint, the conflictual latent state could be label switched, e.g. $k = 0$ or $k = 1$. Moreover, the OMD ensures that latent states (de-)escalate step-wise through adjacent states in the transition matrix (see Fig. 7E).

⁵Fig. 9 in the appendix presents the posterior parameters of a model fitted to the full time range from 2000 to 2020.

7 Applicability to other Models / Domains

The Ordered Matrix Dirichlet as a modeling motif is widely applicable to models with Dirichlet-sampled stochastic matrices. We review other models and discuss application domains as summarized in Fig. 8 in the appendix.

Poisson-Gamma Dynamical System (PGDS). The Poisson-Gamma Dynamical System (Schein et al., 2016a, 2019) has been applied to ICEWS and GDEL (Leetaru and Schrodt, 2013) political events modeling latent states between countries instead of latent communities. It could similarly model ordinal product life cycles (Arvidsson, 2019): the ordinal latent describes the level of product popularity driving purchase counts in different stores per month.

Hidden Markov Model (HMM). Non-ordered, categorical HMMs are widely applied: customer engagement could be modeled as an ordinal latent while purchase counts are naturally ordered and observed (Netzer et al., 2008). The observed change of temperature may be modeled using an ordinal latent indicative of “warming” and “cooling” periods (Perry and Hsu, 2000).

Markov Chain (MC). In Markov Chains, we have a single state transition matrix that could model sleep cycles which transition step-by-step from wake to sleep stages (Pan et al., 2012). Also, rankings in sports or macroeconomics typically involve transitioning to adjacent ranks.

Latent Dirichlet Allocation (LDA). Despite not being a time series model, many topic models feature a Dirichlet-sampled topic-word matrix. The Latent Dirichlet Allocation (LDA) (Blei et al., 2003) is a prominent example. We could semantically order the vocabulary of words, for instance from negative to positive, or boring to funny words. Then, we may want the inferred latent topics to mirror this observed ordering. We can also imagine ordinal topic models beyond textual data such as ordinal topics over ranked athletes from different sports teams.

8 Related Work

Stochastic Matrix Variants To the best of our knowledge, there exists no work constructing row-ordered stochastic matrices. The work by Griffin and Steel (2006) is related to the extent that they modify the weights defining a stick-breaking Dirichlet process to be dependent on co-variables. Relatedly, Massey (1987) studies FSD-constrained Markov processes. The term “ordered Dirichlet” first appears in Yamada and Matsunawa (2000); Huillet (2005) who investigate order statistics of the Dirichlet distribution.

Ordinal Latent Variables A large branch of ordinal methods such as ordered logistic regression (McCullagh,

1980) is based on the concept of latent cut-off points (Chu and Ghahramani, 2005; Virtanen and Girolami, 2015; Terechshenko, 2020; Gouvert et al., 2020). Stoehr et al. (2022) present an ordinal latent variable model that relies on a smooth bijective ordering transform of priors. Their model of conflict intensity incorporates the Goldstein scale, however not a temporal dimension. Netzer et al. (2008) build a Hidden Markov Model with a transition matrix over latent, ordered states representing customer relationship dynamics. They constrain the matrix to adjacent state moves and learn transition probabilities with an ordered logit model. The ordinal characteristics behind the OMD are conceptually different as we tweak a stick-breaking process by repeatedly sorting Beta-sampled vectors.

Latent Conflict Intensity We impose an intensity ordering on event types which sets us apart from O’Connor et al. (2013); Schein et al. (2015, 2016b); Minhas et al. (2016) who assume unordered categorical event types, but still evaluate their latent states against the ordered Goldstein scale in the case of O’Connor et al. (2013). Terechshenko (2020) measure interstate hostility at the country dyad-quarter level. They use an item response theory (IRT) model based on an ordered logistic regression. Treating international relations as latent, unordered states in an Hidden Markov Model is an established modeling idea (Schrodt, 2006; Anders, 2020; Randahl and Vegelius, 2022). Randahl and Vegelius (2022) pre-specify four latent states: peace, conflict, escalation, and de-escalation, and strictly band transitions. This is reminiscent of Kahn’s Escalation Ladder (Kahn, 1962; Davis and Stan, 1984) that defines stages and thresholds of conflict. Neural network-based approaches focus on modeling friend-enemy relationships (Han et al., 2019; Stoehr et al., 2021). The tracing of conflict escalation has also been studied in word embeddings (Kutuzov et al., 2017) and language models (Lefebvre* and Stoehr*, 2022; Hu et al., 2022).

9 Conclusion

This work is fundamentally concerned with imposing a structural constraint onto a (latent) matrix random variable. In doing so, we are facing a trade-off between interpretability and performance which is related, but conceptually different to the bias-variance trade-off in Bayesian model selection (Stoica and Selen, 2004). We are not forfeiting modeling flexibility to reduce model parameters and mitigate overfitting. Instead, the constraint serves the purpose of increasing interpretability of latent states by enforcing a single unique ordering thereof. We test the OMD within a new expressive Dynamic Poisson Tucker Model (DPT) and capture interpretable transition and emission patterns. The OMD may benefit or worsen model fit depending on the true underlying structure of the data. In our experiments, we observe that the OMD serves as a rightful inductive bias making training more robust in few-shot and forecasting settings.

References

- Allman, E. S., Matias, C., and Rhodes, J. A. (2009). Identifiability of parameters in latent structure models with many observed variables. *The Annals of Statistics*, 37(6A).
- Anders, T. (2020). Territorial control in civil wars: Theory and measurement using machine learning. *Journal of Peace Research*, 57(6):701–714.
- Arvidsson, R. (2019). On the use of ordinal scoring scales in social life cycle assessment. *The International Journal of Life Cycle Assessment*, 24(3):604–606.
- Baum, L. E. and Petrie, T. (1966). Statistical Inference for Probabilistic Functions of Finite State Markov Chains. *The Annals of Mathematical Statistics*, 37(6):1554–1563. Publisher: Institute of Mathematical Statistics.
- Bingham, E., Chen, J. P., Jankowiak, M., Obermeyer, F., Pradhan, N., Karaletsos, T., Singh, R., Szerlip, P., Horsfall, P., and Goodman, N. D. (2018). Pyro: Deep Universal Probabilistic Programming. *Journal of Machine Learning Research*.
- Blei, D. M., Ng, A. Y., and Jordan, M. I. (2003). Latent Dirichlet Allocation. *J. Mach. Learn. Res.*, 3(null):993–1022. Publisher: JMLR.org.
- Blondel, M., Teboul, O., Berthet, Q., and Djolonga, J. (2020). Fast Differentiable Sorting and Ranking. *ICML*. Publisher: arXiv Version Number: 2.
- Boschee, E., Lautenschlager, J., O’Brien, S., Shellman, S., Starz, J., and Ward, M. (2015). ICEWS Coded Event Data. Edition: V29 Section: 2015-03-27 14:44:26.045.
- Chu, W. and Ghahramani, Z. (2005). Gaussian Processes for Ordinal Regression. *Journal of Machine Learning Research*, 6:1019–1041.
- Davis, P. K. and Stan, P. J. E. (1984). *Concepts and models of escalation: a report from the Rand Strategy Assessment Center*. Rand, Santa Monica, CA.
- Duane, S., Kennedy, A., Pendleton, B. J., and Roweth, D. (1987). Hybrid Monte Carlo. *Physics Letters B*, 195(2):216–222.
- Gelman, A., Carlin, J. B., Stern, H. S., Dunson, D. B., Vehtari, A., and Rubin, D. B. (2013). *Bayesian Data Analysis*. Chapman and Hall/CRC, 0 edition.
- Gelman, A., Meng, X.-L., and Stern, H. (1996). Posterior Predictive Assessment of Model Fitness via Realized Discrepancies. *Statistica Sinica*, 6(4):733–760. Publisher: Institute of Statistical Science, Academia Sinica.
- Goldstein, J. (1992). A Conflict-Cooperation Scale for WEIS Events Data. *The Journal of Conflict Resolution*, 36(2):369–385.
- Gouvert, O., Oberlin, T., and Févotte, C. (2020). Ordinal Non-negative Matrix Factorization for Recommendation. *2006.01034*, arXiv.
- Griffin, J. E. and Steel, M. F. J. (2006). Order-Based Dependent Dirichlet Processes. *Journal of the American Statistical Association*, 101(473):179–194. Publisher: [American Statistical Association, Taylor & Francis, Ltd.].
- Hadar, J. and Russell, W. R. (1969). Rules for Ordering Uncertain Prospects. *The American Economic Review*, 59(1):25–34. Publisher: American Economic Association.
- Han, X., Choi, E., and Tan, C. (2019). No Permanent Friends or Enemies: Tracking Relationships between Nations from News. In *Proceedings of the 2019 Conference of the North American Chapter of the Association for Computational Linguistics: Human Language Technologies*, volume 1, pages 1660–1676.
- Hillar, C. and Sommer, F. (2011). Ramsey theory reveals the conditions when sparse coding on subsampled data is unique. *arXiv*, 1106.3616.
- Homan, M. D. and Gelman, A. (2014). The No-U-Turn Sampler: Adaptively Setting Path Lengths in Hamiltonian Monte Carlo. *Journal of Machine Learning Research*, 15(1):1593–1623. Publisher: JMLR.org.
- Hu, Y., Hosseini, M., Parolin, E. S., Osorio, J., Khan, L., Brandt, P. T., and D’Orazio, V. J. (2022). ConflIBERT: A Pre-trained Language Model for Political Conflict and Violence. In *Proceedings of the 2022 Conference of the North American Chapter of the Association for Computational Linguistics*.
- Huillet, T. (2005). Unordered and ordered sample from dirichlet distribution. *Annals of the Institute of Statistical Mathematics*, 57(3):597–616.
- Kahn, H. (1962). Kahn’s Escalation Ladder.
- Kalyvas, S. N. (2006). *The Logic of Violence in Civil War*. Cambridge University Press, Cambridge.
- Kutuzov, A., Veldal, E., and Øvreliid, L. (2017). Tracing armed conflicts with diachronic word embedding models. In *Proceedings of the Events and Stories in the News Workshop*, pages 31–36.
- Leetaru, K. and Schrodt, P. (2013). GDELT: Global data on events, location, and tone. In *ISA Annual Convention*.
- Lefebvre*, C. and Stoehr*, N. (2022). Rethinking the Event Coding Pipeline with Prompt Entailment. In *arXiv*, volume 10.48550.
- Massey, W. A. (1987). Stochastic Orderings for Markov Processes on Partially Ordered Spaces. *Mathematics of Operations Research*, 12(2):350–367. Publisher: INFORMS.
- McClelland, C. (1984). World Event/Interaction Survey (WEIS) Project, 1966-1978: Archival Version. type: dataset.
- McCullagh, P. (1980). Regression Models for Ordinal Data. *Journal of the Royal Statistical Society. Series B (Method-*

- ological), 42(2):109–142. Publisher: [Royal Statistical Society, Wiley].
- Minhas, S., Hoff, P. D., and Ward, M. D. (2016). A new approach to analyzing coevolving longitudinal networks in international relations. *Journal of Peace Research*, 53(3):491–505.
- Netzer, O., Lattin, J. M., and Srinivasan, V. (2008). A Hidden Markov Model of Customer Relationship Dynamics. *Marketing Science*, 27(2):185–204.
- O’Connor, B., Stewart, B., and Smith, N. (2013). Learning to Extract International Relations from Political Context. In *Proceedings of the 51st Annual Meeting of the Association for Computational Linguistics*, volume 1, pages 1094–1104.
- Pan, S.-T., Kuo, C.-E., Zeng, J.-H., and Liang, S.-F. (2012). A transition-constrained discrete hidden Markov model for automatic sleep staging. *BioMedical Engineering OnLine*, 11(1):52.
- Perry, C. A. and Hsu, K. J. (2000). Geophysical, archaeological, and historical evidence support a solar-output model for climate change. *Proceedings of the National Academy of Sciences*, 97(23):12433–12438.
- Phan, D., Pradhan, N., and Jankowiak, M. (2019). Composable Effects for Flexible and Accelerated Probabilistic Programming in NumPyro. *arXiv*, 1912.11554.
- Randahl, D. and Vegelius, J. (2022). Predicting Escalating and De-Escalating Violence in Africa Using Markov Models. *International Interactions*, pages 1–17.
- Schein, A., Linderman, S. W., Zhou, M., Blei, D. M., and Wallach, H. (2019). Poisson-Randomized Gamma Dynamical Systems. In *Proceedings of the 33rd International Conference on Neural Information Processing Systems*. Curran Associates Inc., Red Hook, NY, USA.
- Schein, A., Paisley, J., Blei, D. M., and Wallach, H. (2015). Bayesian Poisson Tensor Factorization for Inferring Multilateral Relations from Sparse Dyadic Event Counts. In *Proceedings of the 21th ACM SIGKDD International Conference on Knowledge Discovery and Data Mining, KDD ’15*, pages 1045–1054, New York, NY, USA. Association for Computing Machinery. event-place: Sydney, NSW, Australia.
- Schein, A., Wallach, H., and Zhou, M. (2016a). Poisson-Gamma dynamical systems. In Lee, D., Sugiyama, M., Luxburg, U., Guyon, I., and Garnett, R., editors, *Advances in Neural Information Processing Systems*, volume 29. Curran Associates, Inc.
- Schein, A., Zhou, M., Blei, D. M., and Wallach, H. (2016b). Bayesian Poisson Tucker Decomposition for Learning the Structure of International Relations. In *Proceedings of the 33rd International Conference on International Conference on Machine Learning - Volume 48, ICML’16*, pages 2810–2819. JMLR.org. event-place: New York, NY, USA.
- Schrodt, P. (2008). Kansas Event Data System (KEDS). Edition: V1 Section: 2008-10-10 15:56:53.629.
- Schrodt, P. (2012). CAMEO: Conflict and Mediation Event Observations Event and Actor Codebook. *Parus Analytics*.
- Schrodt, P., Yilmaz, O., Gerner, D., Hermrick, D., Bron, A., Gregory, A., Ingram, A., Jekic, M., McMullen, L., Prather, L., and Pric, T. (2008). Coding Sub-State Actors using the CAMEO (Conflict and Mediation Event Observations) Actor Coding Framework. In *Annual Meeting of the International Studies Association*.
- Schrodt, P. A. (2006). Forecasting Conflict in the Balkans using Hidden Markov Models. In *Programming for Peace*, pages 161–184. Springer Netherlands, Dordrecht.
- Sethuraman, J. (1994). A Constructive Definition of Dirichlet Priors. *Statistica Sinica*, 4(2):639–650. Publisher: Institute of Statistical Science, Academia Sinica.
- Stephens, M. (2000). Dealing with label switching in mixture models. *Journal of the Royal Statistical Society: Series B (Statistical Methodology)*, 62(4):795–809.
- Stoehr, N., Hennigen, L. T., Ahabab, S., West, R., and Cotterell, R. (2021). Classifying Dyads for Militarized Conflict Analysis. In *Proceedings of the 2021 Conference on Empirical Methods in Natural Language Processing (EMNLP)*.
- Stoehr, N., Hennigen, L. T., Valvoda, J., West, R., Cotterell, R., and Schein, A. (2022). An Ordinal Latent Variable Model of Conflict Intensity. In *arXiv*, volume 2210.03971.
- Stoica, P. and Selen, Y. (2004). Model-order selection. *IEEE Signal Processing Magazine*, 21(4):36–47.
- Subakan, Y. C., Traa, J., Smaragdis, P., and Hsu, D. (2015). Method of moments learning for left-to-right Hidden Markov models. In *2015 IEEE Workshop on Applications of Signal Processing to Audio and Acoustics (WASPAA)*, pages 1–5, New Paltz, NY, USA. IEEE.
- Terechshenko, Z. (2020). Hot under the collar: A latent measure of interstate hostility. *Journal of Peace Research*, 57(6):764–776.
- Tucker, L. R. (1964). The extension of factor analysis to three-dimensional matrices. In Gulliksen, H. and Frederiksen, N., editors, *Contributions to mathematical psychology*, pages 110–127. Holt, Rinehart and Winston, New York.
- Virtanen, S. and Girolami, M. A. (2015). Ordinal Mixed Membership Models. *ICML*, pages 588–596.
- Yamada, T. and Matsunawa, T. (2000). Quantitative Approximation to the Ordered Dirichlet Distribution under Varying Basic Probability Spaces. *Annals of the Institute of Statistical Mathematics*, 52(2):197–214.

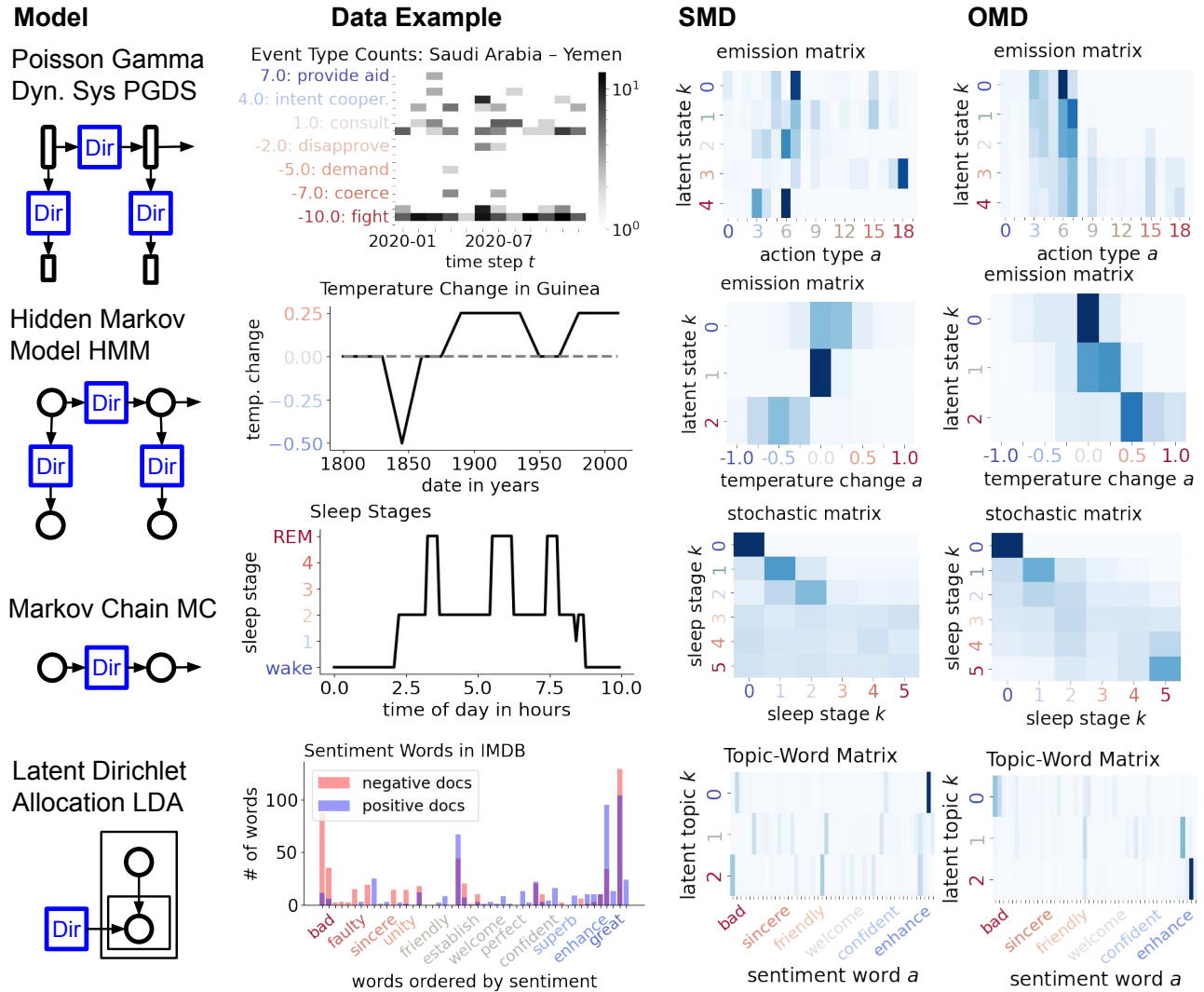


Figure 8: Different models with Dirichlet-sampled latent matrices fitted on data exhibiting ordinal dynamics. The Latent Dirichlet Allocation (LDA) is not a dynamical system, but similarly comprises a stochastic matrix describing word distributions per latent topic. If we order the observed vocabulary of words by the words’ sentiment score, the Ordered Matrix Dirichlet (OMD) can recover topics representative of sentiment levels. In all settings, we find that the OMD yields more easily interpretable stochastic matrices than the Standard Matrix Dirichlet (SMD).

Acknowledgements

We would like to thank the anonymous reviewers, Kevin Du and Lucas Torroba Hennigen for their valuable feedback.

Impact Statement

We emphasize that our models are intended for research purposes and empirical insights. They should not be blindly deployed for automated decision-making processes. The used ICEWS data may contain biases that are potentially reinforced by our modeling assumptions. The experiments with real-world event data in §6.3 were conducted on an NVIDIA TITAN RTX GPU. The experiments with synthetically generated data in §5 can be run on a local M1 CPU with 64 GB of RAM in less than 10 minutes. Limiting factors are the selected hyperparameter sizes for the latent states K and communities C , as well as the number of time series and their length. We discuss further model limitations in §9 and §3.3.

A Expected Value of the Ordered Matrix Dirichlet

The following behavior has been observed:

$$\mathbb{E}[\phi_{11} | \alpha_1 = \dots = \alpha_A] \neq \mathbb{E}[\phi_{KA} | \alpha_1 = \dots = \alpha_A] \quad (7)$$

This is unappealing. Let's get an analytic form for these expectations to understand why and to understand how to set $\alpha_1 \dots \alpha_A$ to get this form of symmetry.

What is the expectation $\mathbb{E}[\phi_{11} | \alpha_1 = \dots = \alpha_A]$? This will involve looking at the *order statistics* of the Beta distribution. From Algorithm 1, we know that ϕ_{11} is drawn

$$P(\phi_{11} | \alpha_1, \dots, \alpha_A) = \text{Beta}^{(1)} \left(\alpha_1, \sum_{a=2}^A \alpha_a \right) \quad (8)$$

where $\text{Beta}^{(k)}(\alpha_1, \alpha_2)$ denotes the k^{th} order statistic of a Beta distribution with parameters α_1 and α_2 . The order statistic of the Beta is known to be:

$$\text{Beta}^{(k)}(\phi; \alpha_1, \alpha_2) = k(1 - \phi)^{\alpha_2 - 1} \phi^{\alpha_1 - 1} I_\phi(\alpha_1, \alpha_2)^{k-1} \left(1 - \frac{I_\phi(\alpha_1, \alpha_2) \Gamma(\alpha_1 + \alpha_2)}{\Gamma(\alpha_1) \Gamma(\alpha_2)} \right)^{n-k} \frac{\Gamma(n+1)}{\Gamma(k+1) \Gamma(n-k+1)} \frac{1}{\beta(\alpha_1, \alpha_2)} \quad (9)$$

$$= \frac{\phi^{\alpha_1 - 1} (1 - \phi)^{\alpha_2 - 1}}{\beta(\alpha_1, \alpha_2)} \left(1 - \frac{I_\phi(\alpha_1, \alpha_2)}{\beta(\alpha_1, \alpha_2)} \right)^{n-k} \left(I_\phi(\alpha_1, \alpha_2) \right)^{k-1} k \binom{n}{k} \quad (10)$$

B Supplementary Technical Details

B.1 Details of the Banded Matrix Dirichlet (BMD).

In this section, we elaborate on the Banded Matrix Dirichlet (BMD) introduced in §3.2. For simplicity, we consider a square matrix $\mathbf{\Pi} \in [0, 1]^{K \times K}$, but the BMD can be non-square as well. We assume that the k^{th} state can only be excited by its directly adjacent states, $(k-1)^{\text{th}}$ and $(k+1)^{\text{th}}$, as well as by itself (Schrodt, 2006; Randahl and Vegelius, 2022). This results in a matrix whose non-zero elements are banded along the diagonal following:

$$\pi_{kk_2} = \begin{cases} \pi_k^{(\nearrow)} & \text{if } k_2 = k + 1 \text{ (escalating)} \\ \pi_k^{(\searrow)} & \text{if } k_2 = k - 1 \text{ (descalating)} \\ \pi_k^{(o)} & \text{if } k_2 = k \text{ (steady)} \\ 0 & \text{otherwise} \end{cases} \quad (11)$$

Finally, we place a Dirichlet prior over the three non-zero elements in each k^{th} row

$$(\pi_k^{(\nearrow)}, \pi_k^{(\searrow)}, \pi_k^{(o)}) \sim \text{Dir}(\alpha_0^{(\nearrow)}, \alpha_0^{(\searrow)}, \alpha_0^{(o)}) \quad (12)$$

Moreover, we can consider a wider bandwidth $b \geq 1$ so that components $k' \in \{k-b, \dots, k+b\}$ all excite k . An example of the full vector might then look like

$$\boldsymbol{\pi}_k = (0, \dots, 0, \pi_k^{(\searrow)}, \pi_k^{(o)}, \pi_k^{(\nearrow)}, 0, \dots, 0) \quad (13)$$

Relevant Links.

Integrated Crisis Early Warning System (ICEWS)

<https://dataverse.harvard.edu/dataverse/icews>

Goldstein Scale

<https://parusanalytics.com/eventdata/cameo.dir/CAMEO.SCALE.txt>

Conflict and Mediation Event Observations (CAMEO)

<https://parusanalytics.com/eventdata/cameo.dir/CAMEO.09b6.pdf>

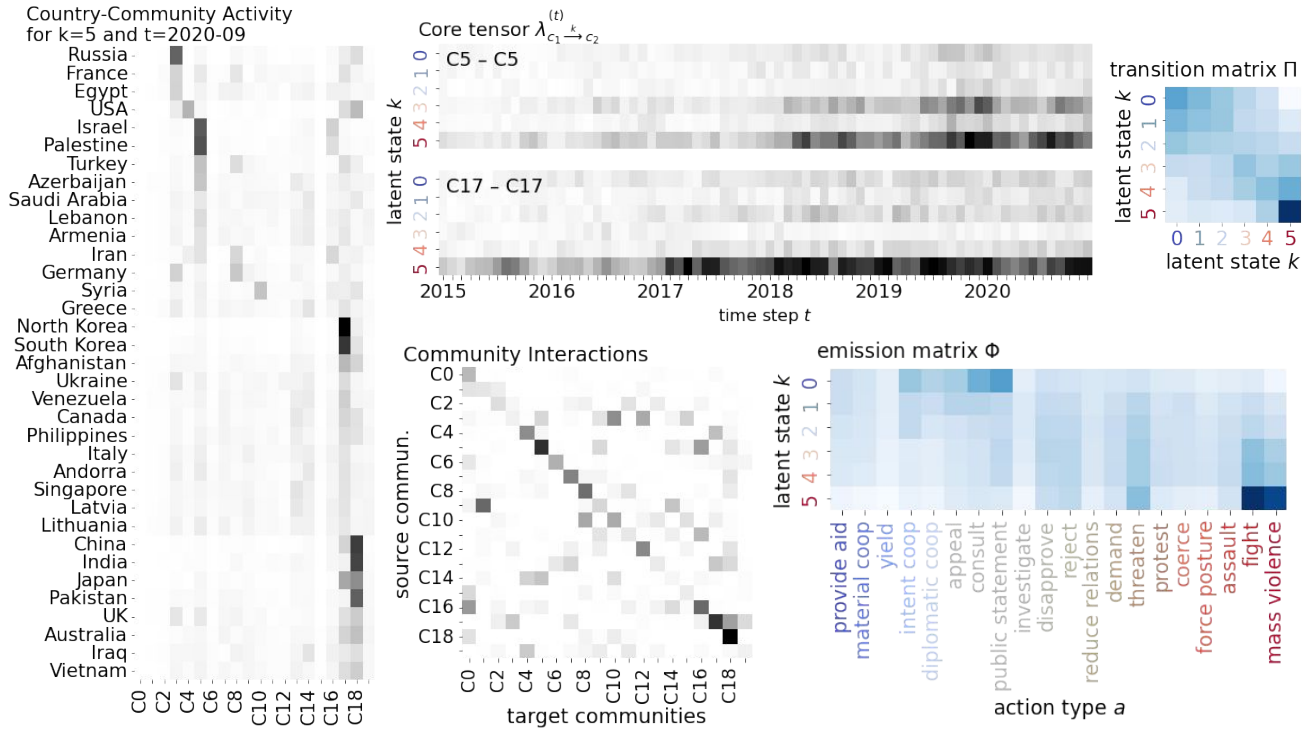


Figure 9: Posterior parameters of Dynamic Poisson Tucker Model, with $K = 6$ latent states and $C = 12$ latent communities, fitted to full temporal range (2000-2020) of ICEWS data. We find that the probability mass of the transition matrix is centered along the diagonal revealing step-wise (de-)escalatory dynamics. Particularly state 5 has high probability representing an “absorbing state” of conflict that is hard to escape. The country-community affiliation matrix Ψ provides no information on whether communities represent allies or enemies per se. To obtain this information, we interact the country-community matrix with the core tensor $\psi_{c_1 i}^{(\rightarrow)} \sum_{c_2=1}^C \sum_{j=1}^J \psi_{c_2 j}^{(\leftarrow)} \lambda_{c_1 \rightarrow c_2}^{(t)}$ for specific choice of k and t .

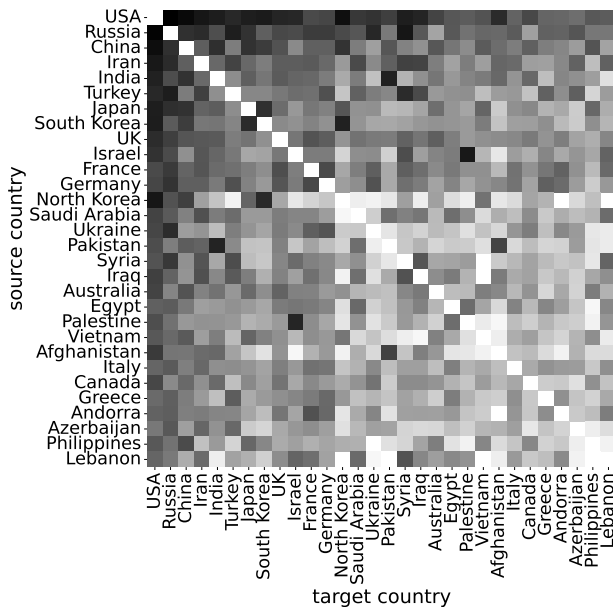


Figure 10: Descriptive statistics showing total number of interactions between countries in ICEWS data from 2015 to 2020. The rows and columns are sorted by the total number of actions a country is involved in. Note that we omit self-targeted actions.

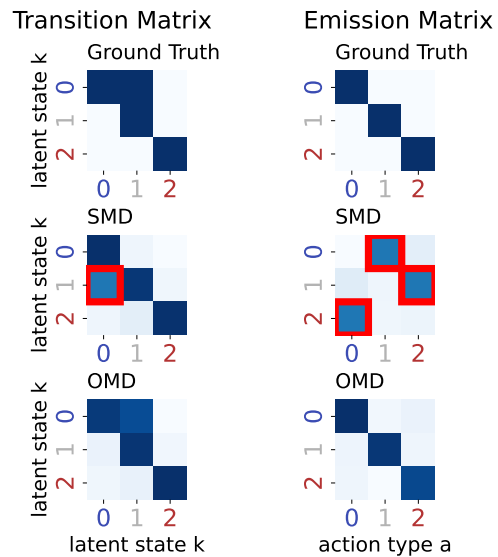


Figure 11: Recovering ground truth structures in transition and emission matrices of a dynamical system. Conventionally, rows are samples independently from a (standard) Dirichlet distribution. This can result in label switching making the latent states (topics) difficult to interpret. This is particularly problematic if states are ordinal, e.g. representing “ally”, “neutral” and “enemy” relations.

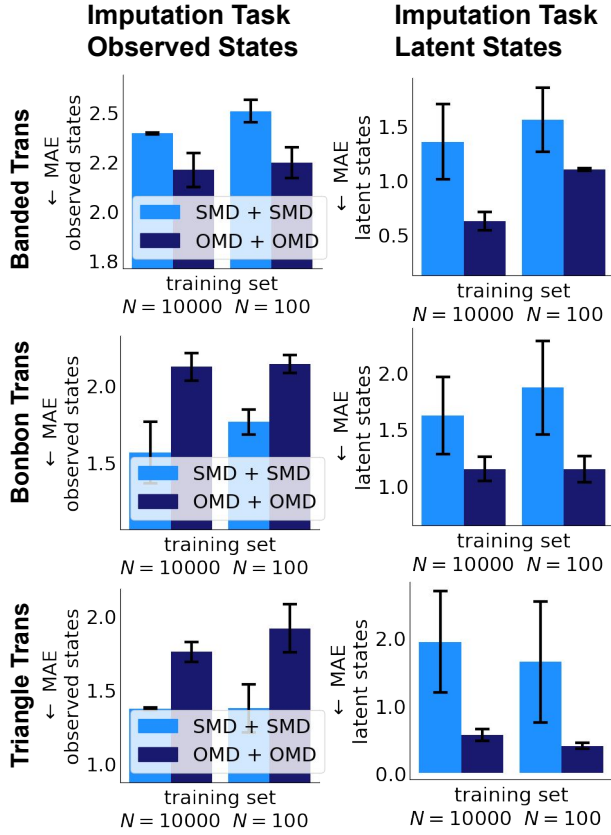


Figure 12: Imputation results of synthetic data experiments. As discussed in §5, we generate time series with different ground truth transition structures: “banded”, “bonbon”, “triangle”. We fit a Hidden Markov Model (HMM) to a train set of these data and evaluate imputation performance on a test set. In contrast to the forecasting experiments (Fig. 4), SMD + SMD outperforms OMD + OMD in two out of three cases on observed states. In contrast to forecasting, imputation does not necessarily require a model with temporal dynamics and the ordered transition matrix does not help. As expected, OMD + OMD performs better at imputing latent states because it circumvents label switching.

action type	action name	Goldstein value
0	provide aid	7.0
1	engage material cooperation	6.0
2	yield	5.0
3	express intent cooperate	4.0
4	engage diplomatic cooperation	3.5
5	appeal	3.0
6	consult	1.0
7	make public statement	0.0
9	investigate	-2.0
10	disapprove	-2.0
11	reject	-4.0
12	reduce relations	-4.0
13	demand	-5.0
14	threaten	-6.0
15	protest	-6.5
16	coerce	-7.0
17	exhibit force posture	-7.2
18	assault	-9.0
19	fight	-10.0
20	unconventional mass violence	-10.0

Figure 13: Ordered CAMEO action types with assigned Goldstein values. We order action types by Goldstein value first and, in case of a tie, by CAMEO ID second.

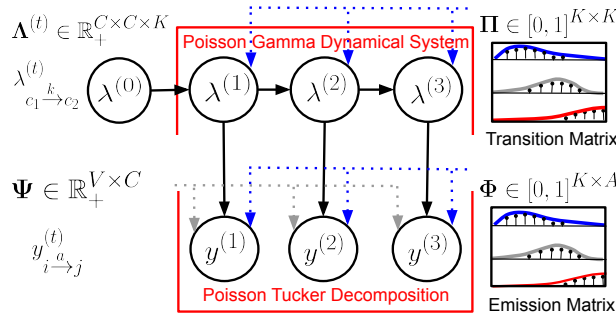


Figure 14: Illustration of the Dynamic Poisson Tucker Model (DPT) that combines the Poisson Tucker Decomposition and the Poisson-Gamma Dynamical System. The 4-mode count tensor of dyadic country interactions Y is factorized into a country-community Ψ and community-interaction core tensor Λ .